

See discussions, stats, and author profiles for this publication at: <https://www.researchgate.net/publication/5816483>

# Relative Hydrophobicity/Hydrophilicity of Fructose, Glucose, Sucrose, and Trehalose as Probed by 1-Propanol: A Differential Approach in Solution Thermodynamics

ARTICLE *in* THE JOURNAL OF PHYSICAL CHEMISTRY B · JANUARY 2008

Impact Factor: 3.3 · DOI: 10.1021/jp074273t · Source: PubMed

---

CITATIONS

11

---

READS

47

3 AUTHORS, INCLUDING:



[Keiko Nishikawa](#)

Chiba University

217 PUBLICATIONS 3,964 CITATIONS

[SEE PROFILE](#)



[Peter Westh](#)

Roskilde University

183 PUBLICATIONS 3,434 CITATIONS

[SEE PROFILE](#)

# Relative Hydrophobicity and Hydrophilicity of Some “Ionic Liquid” Anions Determined by the 1-Propanol Probing Methodology: A Differential Thermodynamic Approach

Hitoshi Kato,<sup>†</sup> Keiko Nishikawa,<sup>‡</sup> and Yoshikata Koga<sup>\*,§</sup>

Graduate School of Science and Technology, Chiba University, Chiba, Japan 263-8522, Graduate School of Advanced Integration Science, Chiba University, Chiba, Japan 263-8522, Department of Chemistry, The University of British Columbia, Vancouver, BC Canada V6T 1Z1, and Research Center for Molecular Thermodynamics, Graduate School of Science, Osaka University, Toyonaka, Osaka 560-0043, Japan

Received: November 14, 2007; In Final Form: December 7, 2007

The excess partial molar enthalpy of 1-propanol (1P),  $H_{1P}^E$ , was experimentally measured in ternary 1P-[NaPF<sub>6</sub>, NaCF<sub>3</sub>SO<sub>3</sub> (OTF) or NaN(SO<sub>2</sub>CF<sub>3</sub>)<sub>2</sub> (TFSI)]-H<sub>2</sub>O system. From the  $H_{1P}^E$  data, the enthalpic 1P–1P interaction function,  $H_{1P-1P}^E$ , which is the compositional derivative of  $H_{1P}^E$ , was evaluated graphically. On addition of the Na salt, the  $x_{1P}$ -dependence pattern of  $H_{1P-1P}^E$  showed a characteristic change. This induced change is used as a probe to elucidate the effect of the sample Na-salt on H<sub>2</sub>O. Because we know the effect of Na<sup>+</sup> from our previous work, we show that each anion works as an amphiphile with hydrophobic and hydrophilic effects. Furthermore, the present method can quantify its relative hydrophobicity and hydrophilicity separately. The results indicate that the relative hydrophobicity ranking was in the order of TFSI<sup>−</sup> > PF<sub>6</sub><sup>−</sup> ≈ OTF<sup>−</sup>, and the hydrophilicity TFSI<sup>−</sup> > PF<sub>6</sub><sup>−</sup> > OTF<sup>−</sup>. Namely, TFSI<sup>−</sup> is the strongest amphiphile with the strongest hydrophobicity and the strongest hydrophilicity among the ionic liquid (IL) anions studied here. Using our earlier similar studies for normal ions, we map their relative hydrophobicity/hydrophilicity scales on a two-dimensional map together with those of the IL ions. The resulting map shows that the typical constituent ions for “ionic liquids” are strong amphiphiles; with more strongly hydrophobic and more strongly hydrophilic propensities than normal ions. Although the number of data points is limited, the melting points of ionic liquids consisting of TFSI<sup>−</sup> with the strongest hydrophobicity and the strongest hydrophilicity within the anions studied here are the lowest.

## Introduction

Ionic liquids (IL's) are attracting a great deal of attention as a new group of compounds.<sup>1–3</sup> Their properties such as nonvolatility, chemical and thermal stability, and high ionic conductivity are very attractive for solvents in the chemical industry; in particular, the low volatility makes it even more attractive for environmental concern. As for the physicochemical interests, the most peculiar nature is their low melting points, in spite of the fact that they consist of cations and anions. For example, 1-butyl-3-methylimidazolium ([bmim]) bis(trifluoromethylsulfonyl)imide (TFSI), one of IL's takes the liquid state even below 0 °C,<sup>4</sup> while the melting point of a typical ionic compound, NaCl, is 801 °C. Generally, IL's absorb moisture from the atmosphere, and their physical properties are often changed by the presence of H<sub>2</sub>O.<sup>5,6</sup> This hygroscopic nature of IL can be an obstacle for use as chemical reaction media, electrolytes, and other various applications. Therefore, the effect of H<sub>2</sub>O on IL is an important information and has been investigated by various methods.<sup>5,6</sup>

Being ionic compounds, the chemistries of their aqueous solutions may be of great interest, just as those of aqueous alkali halides, for example. To this end, we have studied the effects of an IL ion on H<sub>2</sub>O in binary IL–H<sub>2</sub>O systems<sup>7</sup> using a differential thermodynamic methodology.<sup>8–10</sup> Unlike conven-

tional solution thermodynamics, we evaluate the higher-order derivatives of Gibbs function,  $G$ .

By this method, we have elucidated the mixing schemes or the molecular-level processes in aqueous solutions of both electrolytes<sup>11–14</sup> and nonelectrolytes<sup>9,10,15</sup> to unprecedented depth. For binary aqueous 1-propanol (1P), 1P–H<sub>2</sub>O, for example, we experimentally determined the excess partial molar enthalpy of 1P,  $H_{1P}^E$ , which is the second derivative of excess Gibbs function,  $G^E$ . Namely,

$$H_{1P}^E \equiv \left( \frac{\partial H^E}{\partial n_{1P}} \right) \quad (1)$$

where  $H^E$  is the excess enthalpy of the entire system and  $n_{1P}$  is the amount of 1P. As eq 1 suggests,  $H_{1P}^E$  shows the effect of incoming 1P on the total enthalpy of system and hence it signifies the actual enthalpic situation of 1P. We then take one more compositional derivative as

$$H_{1P-1P}^E \equiv N \left( \frac{\partial H_{1P}^E}{\partial n_{1P}} \right) = (1 - x_{1P}) \left( \frac{\partial H_{1P}^E}{\partial x_{1P}} \right) \quad (2)$$

where  $x_{1P}$  is the mole fraction of 1P. As is evident from eq 2,  $H_{1P-1P}^E$  indicates the effect of incoming 1P on the enthalpic situation of existing 1P. Hence,  $H_{1P-1P}^E$  is an indicator of 1P–1P interaction in terms of enthalpy. Using these and other second and third derivative quantities,<sup>9,10,16</sup> we showed that in binary 1P–H<sub>2</sub>O there are three composition regions in each of

\* Corresponding author. E-mail: koga@chem.ubc.ca.

<sup>†</sup> Graduate School of Science and Technology, Chiba University.

<sup>‡</sup> Graduate School of Advanced Integration Science, Chiba University.

<sup>§</sup> The University of British Columbia and Osaka University.

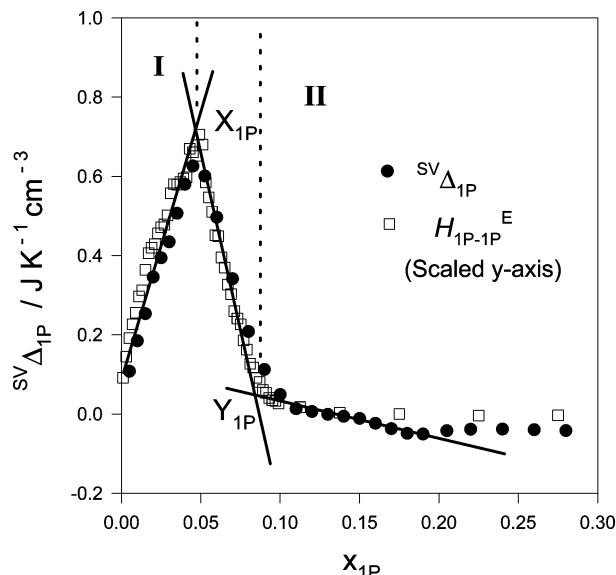


**Figure 1.**  $x_{1P}$  dependencies of the enthalpic 1P–1P interaction function,  $H_{1P-1P}^E$  (open square), and partial molar normalized entropy–volume cross fluctuation of 1P,  $^{SV}\Delta_{1P}$  (filled circle). This graph is taken from ref 16.

which the mixing scheme is qualitatively different from those in the other regions. We call these three mixing schemes from the H<sub>2</sub>O-rich region Mixing Schemes I, II, and III. In the H<sub>2</sub>O-rich region ( $x_{1P} < 0.05$ ), the hydrogen-bond percolation remains intact as in pure H<sub>2</sub>O. Only in this region, “icebergs” are formed around 1P molecules.<sup>17</sup> Namely, 1P molecules locally enhance the hydrogen-bond network of H<sub>2</sub>O in the vicinity of 1P. At the same time, the hydrogen-bond probability of the bulk H<sub>2</sub>O away from 1P is reduced. But the hydrogen bond probability is still high enough that the hydrogen-bond percolation remains intact. We call this mode of mixing Mixing Scheme I, as mentioned above. At the threshold ( $x_{1P} = 0.05$ ), the hydrogen-bond network of the bulk H<sub>2</sub>O loses its bond-percolation nature; that is, the network is no longer connected throughout the entire bulk. In the 1P-rich region where Mixing Scheme III is operative ( $x_{1P} > 0.79$ ),<sup>8,9</sup> 1P molecules form clusters of their own, to which H<sub>2</sub>O molecules interact almost as a single molecule. Mixing Scheme II in the middle region is such that H<sub>2</sub>O-rich clusters and 1P-rich ones are mixed.

As for IL–H<sub>2</sub>O, we found, using the same methodology, that [bmim]BF<sub>4</sub> and [bmim]I dissociate completely in the very H<sub>2</sub>O-rich region below  $x_{IL} < 0.015$  ( $x_{IL}$  is the mole fraction of IL).<sup>7</sup> Some recent studies also suggested that the critical aggregation concentration of [bmim]BF<sub>4</sub> is  $x_{IL} = 0.013$ – $0.017$ .<sup>18–20</sup> In the region,  $0.015 < x_{IL} < 0.5$ , the IL ions seem to start aggregating, and eventually IL molecules cluster together with their own in the IL-rich region,  $x_{IL} > 0.5$ . In this study, we seek the effects of each constituent anions of some IL on H<sub>2</sub>O separately by the 1P-probing methodology developed by us earlier.<sup>11–15,21–24</sup>

For binary 1P–H<sub>2</sub>O, the transition from Mixing Scheme I to II was found to be associated with a peak anomaly as shown in Figure 1.<sup>9,16</sup> We have defined earlier the normalized entropy–volume ( $S$ – $V$ ) cross fluctuation,  $^{SV}\Delta$ , using the thermal expansivity data,  $\alpha_p$ , which is another second derivative.<sup>16,25</sup> We then evaluate the effect of an additional 1P on  $^{SV}\Delta$ , the partial molar normalized  $S$ – $V$  cross fluctuation of 1P,  $^{SV}\Delta_{1P}$ . Because of the putative formation/destruction of ice-like patches in liquid H<sub>2</sub>O, the  $S$ – $V$  cross fluctuation in H<sub>2</sub>O contains a negative contribution, that is, a volume increase could be associated with an entropy decrease. In Figure 1, this  $^{SV}\Delta_{1P}$  data are also plotted.

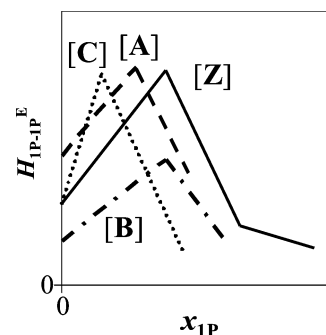


**Figure 2.** Schematic diagram of the  $H_{1P-1P}^E$  pattern. [Z] shows the case for binary 1P–H<sub>2</sub>O. In the presence of a third component S, the resulting  $H_{1P-1P}^E$  pattern shifts as shown by [A] for S = hydrophobic solutes in ternary 1P–S–H<sub>2</sub>O. The pattern indicated by [B] is for S = hydrophilic solutes, and that by [C] for S = hydration centers.

It is evident from the figure that the  $x_{1P}$  dependencies of  $H_{1P-1P}^E$  and  $^{SV}\Delta_{1P}$  are identical to a single scaling factor on the ordinate. This suggests that the enthalpic 1P–1P interaction function,  $H_{1P-1P}^E$ , and the effect of 1P on  $^{SV}\Delta_{1P}$  share the same fundamental cause. Hence, the 1P–1P interaction is H<sub>2</sub>O-mediated and of a long range, as discussed at some length earlier.<sup>16</sup> Thus, the initial increase in  $^{SV}\Delta_{1P}$  (or  $H_{1P-1P}^E$ ) traces the process of decrease in the negative contribution in  $^{SV}\Delta$ . Therefore, we could follow the manner in which the bulk H<sub>2</sub>O is modified by the addition of 1P, by the behavior of  $H_{1P-1P}^E$  (or  $^{SV}\Delta_{1P}$ ).

On the basis of this finding, we devised the 1P probing methodology. We determine  $H_{1P-1P}^E$  in ternary 1P–sample-(S)–H<sub>2</sub>O systems. As long as the mole fraction of sample,  $x_S^0$ , is not high enough to destroy the integrity of H<sub>2</sub>O completely, the  $H_{1P-1P}^E$  pattern makes some quantitative changes depending on the nature and the amount of S, while the basic peak pattern is retained. Those induced changes of the  $H_{1P-1P}^E$  peak pattern in the presence of S will provide how S modifies H<sub>2</sub>O. We have calibrated this methodology earlier by using as S, 2-propanol<sup>26</sup> (an equal hydrophobe as 1P), urea<sup>27</sup> (a typical hydrophile), and 1,2-propendiol<sup>13</sup> (an amphiphile) and studied their effects on the  $H_{1P-1P}^E$  pattern in 1P–S–H<sub>2</sub>O. Figure 2 summarizes the results. If S is equally hydrophobic as 1P [A], then the peak shifts parallel to the left (west), keeping the height unchanged, and making the value of  $H_{1P-1P}^E$  at the starting point ( $x_{1P} = 0$ ) increase. In the case of S being a hydrophile [B], the value of  $H_{1P-1P}^E$  at point X decreases (or point X shifts to the south) and the locus of  $x_{1P}$  at point X remains unchanged. We argued with a support from a theoretical work (Idrissi et al., ref 28) that urea forms hydrogen bonds to the existing hydrogen bond network directly. By so doing, urea retards the degree of fluctuation in the whole aqueous solution, by breaking the H donor/acceptor symmetry of liquid H<sub>2</sub>O. For an amphiphilic sample S, its effect appears as a combination of [A] and [B]. Namely, the locus of point X shifts to the left by the effect of its hydrophobic moiety. At the same time, its hydrophilic part makes the value of  $H_{1P-1P}^E$  decrease. As a result, point X shifts to the southwest. We also applied the same methodology for S=NaCl.<sup>11</sup> It turned out that the results are as shown as [C] in Figure 2. The  $H_{1P-1P}^E$  pattern appears squashed to the left without changing the values of  $H_{1P-1P}^E$  at the start,  $x_{1P} = 0$ , and at point X. We thus suggested that NaCl hydrates a number of H<sub>2</sub>O molecules making them unavailable for 1P to interact; that is, NaCl is a hydration center.<sup>11,14</sup> From the left shift of point X for a unit increase in  $x_S^0$ , we found the

hydration number of NaCl to be  $7.5 \pm 0.6$ . From the fact that the values of  $H_{1P-1P}^E$  at point X as well as at the start remain unchanged, we concluded that the bulk  $H_2O$  away from the hydration shell remains unperturbed by the presence of NaCl. Although the “iceberg” formed around a hydrophobe is in effect a hydration shell, the hydrogen bonds are complete within “iceberg”, with concomitant reduction of the hydrogen-bond probability of bulk  $H_2O$  away from “icebergs”. Here for NaCl, we have no information on whether or not the hydrogen bonds are complete within the hydration shell for  $Na^+$  for example. Nonetheless, both hydrophobes and hydration centers cause point X of the  $H_{1P-1P}^E$  pattern to shift westward. A first-principle molecular dynamics study also showed that the  $Na^+$  ion hydrates 5.2 molecules of  $H_2O$  and leaves the bulk  $H_2O$  away from the hydration shell unperturbed (White et al., ref 29). The fact that the hydration number for  $Na^+$  is about 5 gains some more recent theoretical<sup>30</sup> and experimental<sup>31,32</sup> support. Hence, we assign 5.2 to the hydration number for  $Na^+$ . Accordingly,  $Cl^-$  hydrates  $2.3 \pm 0.6$  molecules of  $H_2O$  and leaves the bulk  $H_2O$  away from the hydration shell unperturbed.

Here, we use the same 1P-probing methodology, to the  $Na^+$  salt of some anions that are common in typical ionic liquids,  $PF_6^-$ ,  $CF_3SO_3^-$  (OTF<sup>-</sup>), and  $N(SO_2CF_3)_2^-$  (TFSI<sup>-</sup>), collectively represented by  $IL^-$ . Because the effect of  $Na^+$  is known, we seek how  $IL^-$  modifies  $H_2O$  within Mixing Scheme I. As will become evident below, the  $x_{1P}$ -dependence of  $H_{1P-1P}^E$  retains a peak pattern in the presence of  $Na^+IL^-$  within the range of its initial mole fraction,  $x_S^0$  studied here, which assures that the aqueous solutions of  $Na^+IL^-$  are still in Mixing Scheme I. Thus, the induced shift of the peak, point X, would suggest how the sample  $Na^+IL^-$  modifies  $H_2O$ . Assuming that  $Na^+IL^-$  is completely dissociated, the effect of  $Na^+$  and that of  $IL^-$  can be separated with the previous knowledge about the former. It turned out that all of the  $IL^-$  ions studied here work as amphiphiles with different degrees of hydrophobic and hydrophilic effects. We thus could evaluate the relative strength of hydrophobic and hydrophilic effects of each anion in terms of the rate of the induced west- and southward shifts of point X by a unit addition of  $IL^-$ . We stress that our usage of “hydrophobic” and “hydrophilic” is limited strictly in this sense within our 1P-probing methodology.

In our previous paper,<sup>33</sup> we applied the same methodology and discussed the effect of [bmim]Cl on the molecular organization of  $H_2O$ . By knowing the effect of  $Cl^-$ , it was shown that the [bmim]<sup>+</sup> ion acts as an amphiphile also. The carbon atom between two nitrogens of [bmim]<sup>+</sup> is known to be a proton-donor,<sup>34</sup> which interacts with the hydrogen-bond network directly. Therefore, the hydrophilic part as well as the hydrophobic moiety of butyl chain brings about the net amphiphilic nature.

## Experimental Section

For determining  $H_{1P}^E$ , a homemade titration calorimeter of a similar design to an LKB Bromma 8700 was used.<sup>35</sup> Briefly, about 5 mol of S- $H_2O$  solution was measured in a titration cell, into which about 10 mmol of 1P ( $\delta n_{1P}$ ) is titrated using a buret and the thermal response,  $\delta q_p$  was determined.  $H_{1P}^E$  is approximated by  $\delta q_p/\delta n_{1P}$ . This ratio of the titrant to the titrand was earlier checked small enough for an acceptable approximation.<sup>35</sup> The uncertainty in  $H_{1P}^E$  is estimated as  $\pm 0.03 \text{ kJ mol}^{-1}$ . The temperature of the system is kept at  $25 \pm 0.001 \text{ }^\circ\text{C}$  in a water bath.

$NaPF_6$  (Wako),  $NaOTF$  (Wako),  $NaTFSI$  (JEMCO), and 1-propanol (Wako, special grade, >99.5%) were used as supplied.

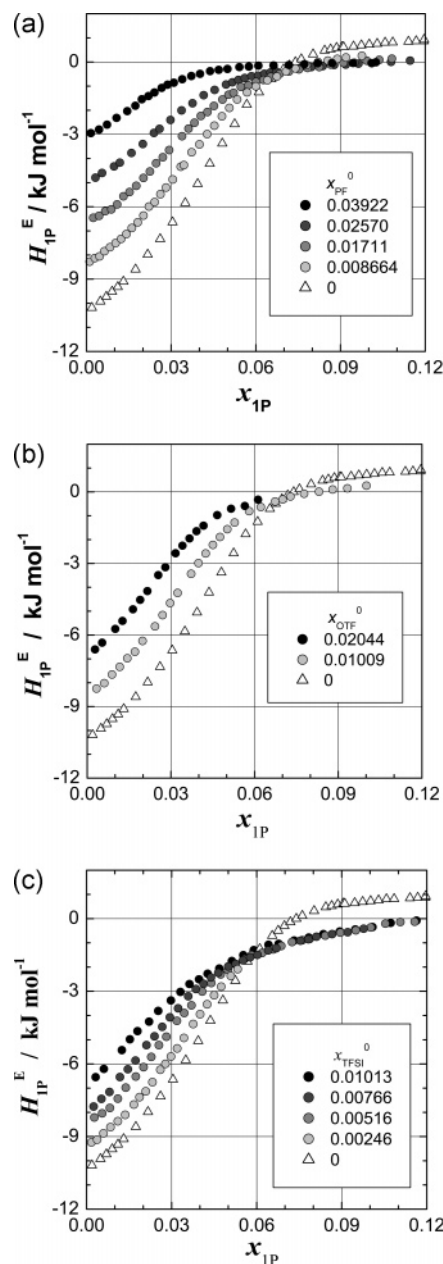


**Figure 3.** Excess partial molar enthalpy,  $H_{1P}^E$ , against  $x_{1P}$ , at 25  $^\circ\text{C}$ . (a) For 1P- $NaPF_6$ - $H_2O$ , (b) 1P- $NaOTF$ - $H_2O$ , and (c) 1P- $NaTFSI$ - $H_2O$ .

S- $H_2O$  solutions were made gravimetrically immediately prior to use. 1-Propanol was kept in a dry nitrogen atmosphere during the course of the measurements.

## Results and Discussion

Figure 3a-c show the  $H_{1P}^E$  data for the ternary systems, 1P-{ $NaPF_6$ ,  $NaOTF$ , and  $NaTFSI$ }- $H_2O$ , respectively. From the  $H_{1P}^E$  data, we evaluated  $H_{1P-1P}^E$  graphically by eq 2, without resorting to any model system. The detail of graphical differentiation is given earlier.<sup>22</sup> The results are shown in Figure 4. The uncertainty in  $H_{1P-1P}^E$  inevitably increases but is estimated to be not more than  $\pm 10 \text{ kJ mol}^{-1}$ .<sup>22</sup> It is clear from the figure that point X of each system shifts to the southwest, suggesting amphiphilic propensity. However, the west shift will contain the hydration effect by  $Na^+$ . Figure 5 shows the changes in the value of  $x_{1P}$  at point X for each sample as a function of  $x_S^0$ . Hence, the slope (negative) in the figure could be used as



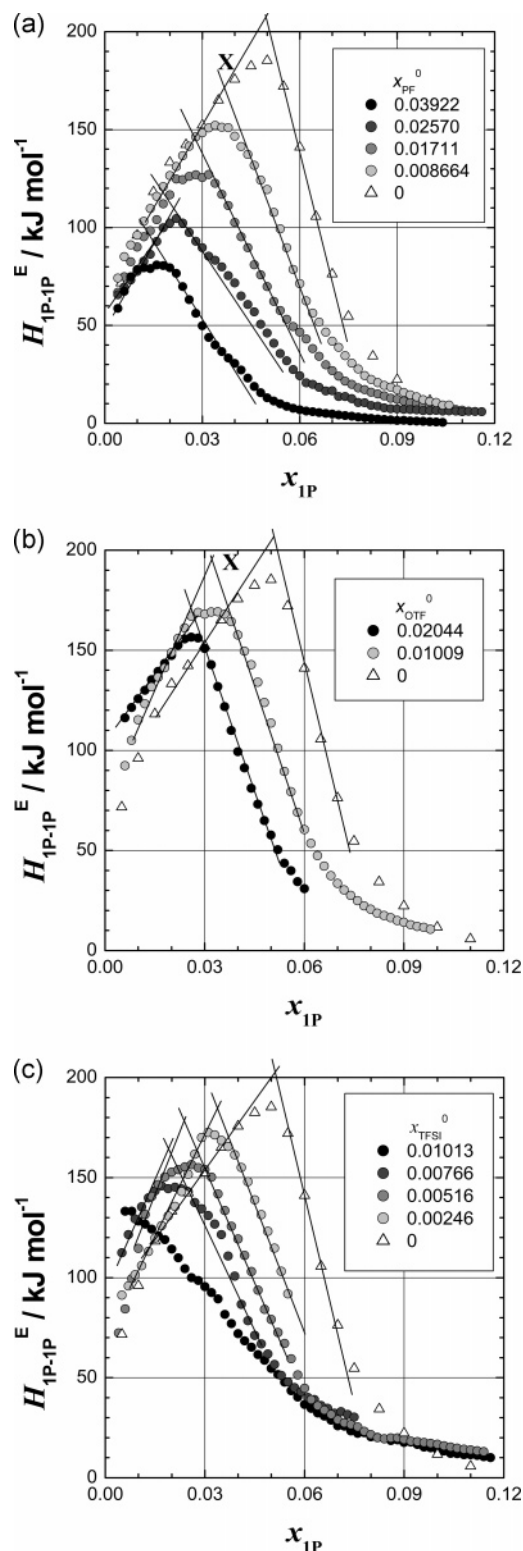


**Figure 4.**  $x_{1P}$  dependencies of the 1P-1P enthalpic interaction,  $H_{1P-1P}^E$ . (a) For 1P-NaPF<sub>6</sub>-H<sub>2</sub>O, (b) 1P-NaOTf-H<sub>2</sub>O, and (c) 1P-NaTFSI-H<sub>2</sub>O.

a relative hydrophobicity index; that is, the stronger the hydrophobicity, the more negative the slope. It indicates the degree of the west shift induced by adding a unit amount of salts. In Figure 5, the west shift due to hydration by Na<sup>+</sup> is also shown as a broken line. Hence, each sample's hydrophobicity is evaluated from slopes in Figure 5 minus that for Na<sup>+</sup>. From these negative slopes, therefore, the order of the relative hydrophobicity is TFSI<sup>-</sup> > PF<sub>6</sub><sup>-</sup> ≈ OTF<sup>-</sup>.

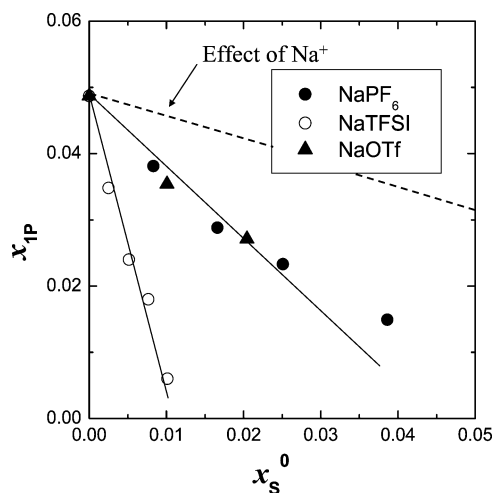


**Figure 5.** Mixing scheme boundary for 1P-S-H<sub>2</sub>O, which is the value of  $x_{1P}$  at point X against various initial mole fraction of the mixed solvent,  $x_s^0$ . Broken line indicates the contribution of the hydration of Na<sup>+</sup>.

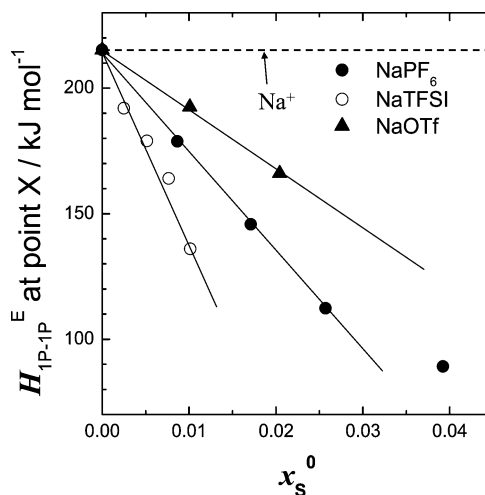


**Figure 6.** Locus of point X in terms of  $H_{1P-1P}^E$  against  $x_s^0$  in ternary 1P-S-H<sub>2</sub>O. Na<sup>+</sup> has no effect on  $H_{1P-1P}^E$  at point X (broken line).

The loci of point X in terms of  $H_{1P-1P}^E$  are plotted in Figure 6. Note that Na<sup>+</sup> does not change the height of point X. Therefore, the negative slope in this figure indicates the hydrophilic effect of each IL anion. This slope-ranking then becomes TFSI<sup>-</sup> > PF<sub>6</sub><sup>-</sup> > OTF<sup>-</sup>. Namely, TFSI<sup>-</sup>, a typical ionic liquid anion, is an amphiphile with the strongest hydrophobic as well as hydrophilic propensities among the anions studied here.

We earlier applied the same methodology to study the effect of various normal ions on H<sub>2</sub>O. From the equivalent plots as Figure 5 and 6, we can evaluate the relative hydrophobicity/hydrophilicity indices for these normal ions. Figure 7 shows such plots for 16 ions including [bmim]<sup>+</sup>,<sup>33</sup> PF<sub>6</sub><sup>-</sup>, OTF<sup>-</sup>, and TFSI<sup>-</sup>. The abscissa of Figure 7 is the slopes (negative) of Figure 5 and equivalent figures for other normal ions. As mentioned above, both hydrophobes and hydration centers make point X shift westward. Therefore, both are plotted on the abscissa. The ordinate is the slopes (negative) of Figure 6 and equivalent figures. H<sub>2</sub>O itself is placed at the origin because S = H<sub>2</sub>O in the 1P-S-H<sub>2</sub>O system would not cause any shift in point X. As for normal ions studied so far, only acetate<sup>-</sup> (OAc<sup>-</sup>)<sup>13</sup> showed a hydrophobic effect. F<sup>-</sup>,<sup>14</sup> Cl<sup>-</sup>,<sup>14</sup> Na<sup>+</sup>,<sup>11,14</sup> Ca<sup>2+</sup>,<sup>12</sup> and NH<sub>4</sub><sup>+</sup><sup>12</sup> act as a hydration center. Alternatively,

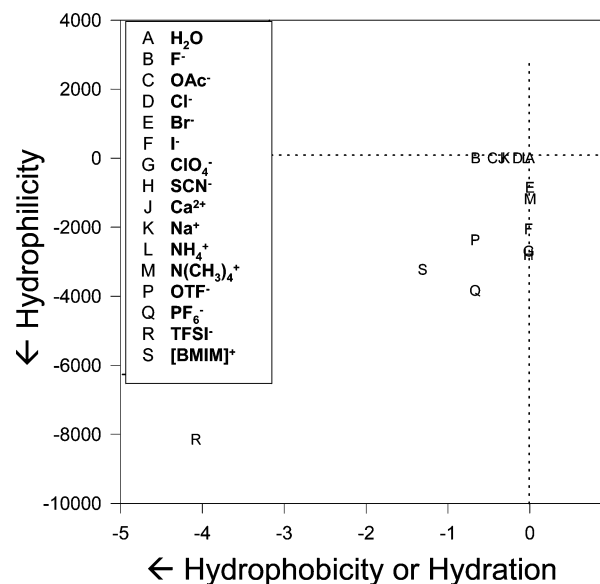


**Figure 7.** Relative hydrophobicity and hydrophilicity map for various ions including four IL ions. H<sub>2</sub>O (A) is at the origin. Hydrophobes and hydration centers cause the locus to shift westward from the origin, and hydrophiles southward. For hydrophobe, C: acetate (OAc<sup>-</sup>). For hydration center, B: F<sup>-</sup>, D: Cl<sup>-</sup>, J: Ca<sup>2+</sup>, K: Na<sup>+</sup>, L: NH<sub>4</sub><sup>+</sup>. For hydrophiles, E: Br<sup>-</sup>, F: I<sup>-</sup>, G: ClO<sub>4</sub><sup>-</sup>, H: SCN<sup>-</sup>, M: N(CH<sub>3</sub>)<sub>4</sub><sup>+</sup> (TMA<sup>+</sup>). For amphiphiles, P: OTF<sup>-</sup>, Q: PF<sub>6</sub><sup>-</sup>, R: TFSI<sup>-</sup>, S: [bmim]<sup>+</sup>.

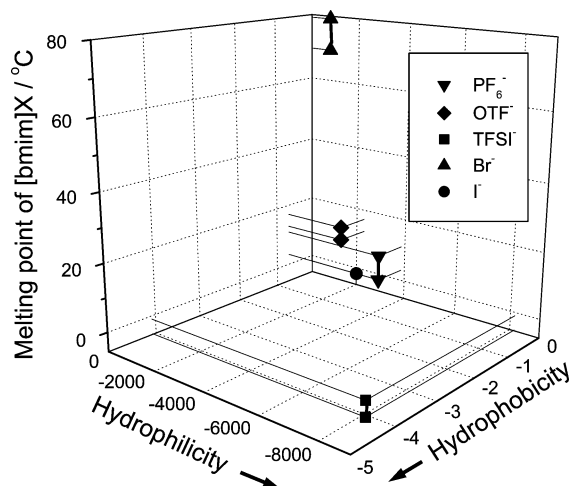


**Figure 8.** Melting points of [bmim]<sup>+</sup> salts with IL anions against the relative anion hydrophobicity/hydrophilicity indices. The melting points are taken from ref 36 (max) and ref 37 (min) for PF<sub>6</sub><sup>-</sup>, ref 4 (max) and ref 36 (min) for OTF<sup>-</sup>, ref 40 (max) and ref 38 (min) for TFSI<sup>-</sup>, ref 42 (max) and ref 43 (min) for Br<sup>-</sup>, and ref 45 for I<sup>-</sup>.

Br<sup>-</sup>,<sup>14</sup> I<sup>-</sup>,<sup>14</sup> ClO<sub>4</sub><sup>-</sup>,<sup>24</sup> SCN<sup>-</sup>,<sup>13</sup> and N(CH<sub>3</sub>)<sub>4</sub><sup>+</sup> (TMA<sup>+</sup>)<sup>12</sup> were found hydrophilic and are placed on the ordinate because they all show no sign of hydrophobicity. It is clear that IL ions are spread out to the southwest, indicating that they are all amphiphiles with strong hydrophobic and equally strong hydrophilic moieties.

Although it is premature to generalize with a limited number of IL ions studied here, this relative hydrophobicity/hydrophilicity index may characterize ions of ionic liquids. We may be tempted to suggest that the direction (i.e., the southwest) and the distance from the origin may be an important factor for the “IL-likeness” of each ion. In this context, TFSI<sup>-</sup> is the most IL-like anion within the present study. It is known that the ionic liquids with TFSI<sup>-</sup> tend to have low viscosities and low melting points. Figure 8 shows the available melting points of [bmim]<sup>+</sup>

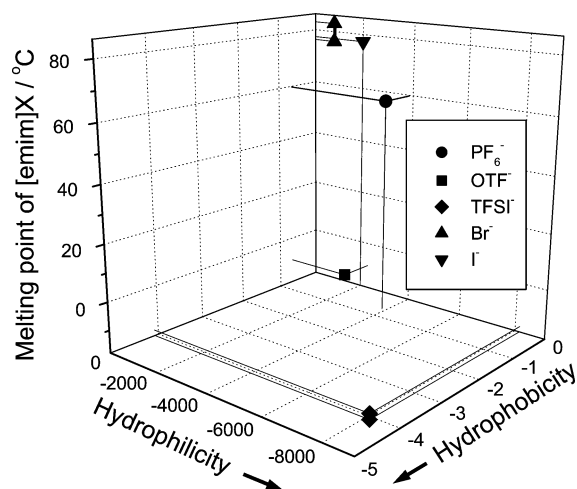


**Figure 9.** Melting points of [emim]<sup>+</sup> salts with IL anions against the relative anion hydrophobicity/hydrophilicity indices. The melting points are taken from ref 46 (max) and ref 37 (min) for PF<sub>6</sub><sup>-</sup>, ref 47 for OTF<sup>-</sup>, ref 40 (max) and ref 41 (min) for TFSI<sup>-</sup>, ref 48 (max) and ref 44 (min) for Br<sup>-</sup>, and ref 45 for I<sup>-</sup>.

ionic liquids with PF<sub>6</sub><sup>-</sup>,<sup>4,36–39</sup> OTF<sup>-</sup>,<sup>4,36</sup> TFSI<sup>-</sup>,<sup>36,38,40,41</sup> Br<sup>-</sup>,<sup>19,42–44</sup> and I<sup>-</sup><sup>45</sup> on the relative hydrophobicity/hydrophilicity map of counter anions. Figure 9 shows the same for 1-ethyl-3-methylimidazolium<sup>+</sup>, [emim]<sup>+</sup>.<sup>36,37,40–42,44,46–48</sup> The available melting points seem to be dependent on the method and the purity of the sample. For such cases, the maximum and the minimum values available in the literature are shown in both figures. Nonetheless, both TFSI<sup>-</sup> salts show the lowest melting points in both figures, that is, the strongest “IL-likeness” within the present study. It is generally accepted that ionic liquids have low melting points because of a large polarity and nonpolarity of constituent ions and the contribution from Coulombic attraction is obscured by other effects due to polarity and nonpolarity coexisting within each ion. The present relative hydrophobicity/hydrophilicity map may serve to quantify such effects.

**Acknowledgment.** This research was supported by the Grant-in-Aid for Scientific Research (No. 17073002) in Priority Area “Science of Ionic Liquids” (Area No. 452) from the Ministry of Education, Culture, Sports, Science and Technology, Japan. We also thank Mr. T. Honda (JEMCO) for synthesizing NaTFSI for the present study.

**Supporting Information Available:** Table SUP of the excess partial molar enthalpy of 1P,  $H_{1P}^E$ , in 1P–S–H<sub>2</sub>O at 25 °C, for S = NaPF<sub>6</sub>, NaOTF, and NaTFSI. This material is available free of charge via the Internet at <http://pubs.acs.org>.

## References and Notes

- (1) Rogers, R. D.; Seddon, K. R. *Ionic Liquids – Industrial Applications for Green Chemistry*; A.C.S. Symposium Series 818, American Chemical Society: Washington, D.C., 2002.
- (2) Wasserscheid, P.; Welton, T. *Ionic Liquids in Synthesis*; Wiley-VCH: Weinheim, 2003.
- (3) Shobukawa, H.; Tokuda, H.; Susan, M. A. B. H.; Watanabe, M. *Electrochim Acta* **2005**, *50*, 3872.
- (4) Tokuda, H.; Tsuzuki, S.; Susan, M. A. B. H.; Hayamizu, K.; Watanabe, M. *J. Chem. Phys. B* **2006**, *110*, 19593.
- (5) Seddon, K. R.; Stark, A.; Torres, M.-J. *Pure Appl. Chem.* **2000**, *72*, 2275.
- (6) Anthony, J. L.; Maginn, E. J.; Brennecke, J. F. *J. Phys. Chem. B* **2001**, *105*, 10942.
- (7) Katayanagi, H.; Nishikawa, K.; Shimozaki, H.; Miki, K.; Westh, P.; Koga, Y. *J. Phys. Chem. B* **2004**, *108*, 19451.
- (8) Koga, Y. *Solution Thermodynamics and its Application to Aqueous Solutions: A Differential Approach*; Elsevier: Amsterdam, 2007.

- (9) Koga, Y. *J. Phys. Chem.* **1996**, *100*, 5172.
- (10) Koga, Y. *Netsusokutei (J. Jpn. Soc. Cal., Therm. Anal.)* **2003**, *30*, 54. Available in a pdf form on request to the author (koga@chem.ubc.ca).
- (11) Matsuo, H.; To, E. C. H.; Wong, D. C. Y.; Sawamura, S.; Taniguchi, Y.; Koga, Y. *J. Phys. Chem. B* **1999**, *103*, 2981.
- (12) Koga, Y.; Katayanagi, H.; Davies, J. V.; Kato, H.; Nishikawa, K.; Westh, P. *Bull. Chem. Soc. Jpn.* **2006**, *79*, 1347.
- (13) Koga, Y.; Westh, P.; Davies, J. V.; Miki, K.; Nishikawa, K.; Katayanagi, H. *J. Phys. Chem. A* **2004**, *108*, 8533.
- (14) Westh, P.; Kato, H.; Nishikawa, K.; Koga, Y. *J. Phys. Chem. A* **2006**, *110*, 2072.
- (15) Parsons, M. T.; Koga, Y. *J. Phys. Chem. B* **2002**, *106*, 7090.
- (16) Koga, Y. *Can. J. Chem.* **1999**, *77*, 2039.
- (17) Koga, Y.; Nishikawa, K.; Westh, P. *J. Phys. Chem. A* **2004**, *108*, 3873.
- (18) Bowers, J.; Butts, C. P.; Martin, P. J.; Vergara-Gutierrez, M. C.; Heenan, R. K. *Langmuir* **2004**, *20*, 2191.
- (19) Wang, J.; Wang, H.; Zhang, S.; Zhang, H.; Zhao, Y. *J. Phys. Chem. B* **2007**, *111*, 6181.
- (20) Singh, T.; Kumar, A. *J. Phys. Chem. B* **2007**, *111*, 7843.
- (21) Miki, K.; Westh, P.; Koga, Y. *J. Phys. Chem. B* **2005**, *109*, 19536.
- (22) Parsons, M. T.; Westh, P.; Davies, J. V.; Trandum, Ch.; To, E. C. H.; Chiang, W. M.; Yee, E. G. M.; Koga, Y. *J. Solution Chem.* **2001**, *30*, 1007.
- (23) Koga, Y. *J. Therm. Anal. Cal.* **2002**, *69*, 705.
- (24) Koga, Y.; Westh, P.; Nishikawa, K. *J. Phys. Chem. A* **2004**, *108*, 1635.
- (25) Koga, Y.; Westh, P.; Sawamura, S.; Taniguchi, Y. *J. Chem. Phys.* **1996**, *105*, 2028.
- (26) Hu, J.; Chiang, W. M.-D.; Westh, P.; Chen, D. H. C.; Haynes, C. A.; Koga, Y. *Bull. Chem. Soc. Jpn.* **2001**, *74*, 809.
- (27) To, E. C. H.; Hu, J.; Haynes, C. A.; Koga, Y. *J. Phys. Chem. B* **1998**, *102*, 10958.
- (28) Idrissi, A.; Bartolini, P.; Ricci, M.; Righini, R. *Phys. Chem. Chem. Phys.* **2003**, *5*, 4666.
- (29) White, J. A.; Schwegler, E.; Galli, G.; Gygi, F. *J. Chem. Phys.* **2000**, *113*, 4668.
- (30) Varma, S.; Rempe, S. B. *Biophys. Chem.* **2006**, *124*, 192.
- (31) Ansell, S.; Barnes, A. C.; Mason, P. E.; Neilson, G. W.; Ramos, S. *Biophys. Chem.* **2006**, *124*, 171.
- (32) Koga, Y. *Solution Thermodynamics and its Application to Aqueous Solutions: A Differential Approach*; Elsevier: Amsterdam, 2007; pp 211–215.
- (33) Miki, K.; Westh, P.; Nishikawa, K.; Koga, Y. *J. Phys. Chem. B* **2005**, *109*, 9014.
- (34) Hunt, P. A. *J. Phys. Chem. B* **2007**, *111*, 4844.
- (35) Koga, Y. *Can. J. Chem.* **1988**, *66*, 1187.
- (36) Fredlake, C. P.; Crosthwaite, J. M.; Hert, D. G.; Aki, S. N. V. K.; Brennecke, J. F. *J. Chem. Eng. Data* **2004**, *49*, 954.
- (37) Domanska, U.; Marciniak, A. *J. Chem. Eng. Data* **2003**, *48*, 451.
- (38) Troncoso, J.; Cerdeirina, C. A.; Sanmamed, Y. A.; Romani, L.; Rebelo, L. P. N. *J. Chem. Eng. Data* **2006**, *51*, 1856.
- (39) Domanska, U.; Mazurowska, L. *Fluid Phase Equilib.* **2004**, *221*, 73.
- (40) MacFarlane, D. R.; Meakin, P.; Amini, N.; Forsyth, M. *J. Phys.: Condens. Matter* **2001**, *13*, 8257.
- (41) Tokuda, H.; Hayamizu, K.; Ishii, K.; Susan, M. A. B. H.; Watanabe, M. *J. Phys. Chem. B* **2005**, *109*, 6103.
- (42) Lozinskaya, E. I.; Shaplov, A. S.; Kotseruba, M. V.; Komarova, L. I.; Lyssenko, K. A.; Antipin, M. Y.; Golovanov, D. G.; Vygodskii, Y. S. *J. Polym. Sci., Part A: Polym. Chem.* **2006**, *44*, 380.
- (43) Golovanov, D. G.; Lyssenko, K. A.; Antipin, M. Y.; Vygodskii, Y. S.; Lozinskaya, E. I.; Shaplov, A. S. *Cryst. Growth Des.* **2005**, *5*, 337.
- (44) Turner, E. A.; Pye, C. C.; Singer, R. D. *J. Phys. Chem. A* **2003**, *107*, 2277.
- (45) Nakakoshi, M.; Shiro, M.; Fujimoto, T.; Machinami, T.; Seki, H.; Tashiro, M.; Nishikawa, K. *Chem. Lett.* **2006**, *35*, 1400.
- (46) Wong, D. S. H.; Chen, J. P.; Chang, J. M.; Chou, C. H. *Fluid Phase Equilib.* **2002**, *194*, 1089.
- (47) Bennett, M. D.; Leo, D. J. *Sens. Actuators, A* **2004**, *115*, 79.
- (48) Liao, J.-H.; Wu, P.-C.; Huang, W.-C. *Cryst. Growth Des.* **2006**, *6*, 1062.